

LATERAL HANDLING IMPROVEMENT WITH DYNAMIC CURVATURE CONTROL FOR AN INDEPENDENT REAR WHEEL DRIVE EV

Youngjin Jang¹⁾, Minyoung Lee²⁾, In-Soo Suh^{3)*} and Kwanghee Nam⁴⁾

¹⁾Electric Power Conversion Control Engineering Design Team, Hyundai-Kia Motor, 150 Hyundaiyeonguso-ro, Namyang-eup, Hwaseong-si, Gyeonggi 18280, Korea

²⁾Department of Mechanical Engineering, KAIST, Daejeon 34141, Korea

³⁾Graduate School for Green Transportation, KAIST, Daejeon 34141, Korea

⁴⁾Department of Electrical and Electronics, POSTECH, Gyeongbuk 37673, Korea

(Received 7 August 2015; Revised 19 December 2015; Accepted 27 June 2016)

ABSTRACT–The integrated longitudinal and lateral dynamic motion control is important for four wheel independent drive (4WID) electric vehicles. Under critical driving conditions, direct yaw moment control (DYC) has been proved as effective for vehicle handling stability and maneuverability by implementing optimized torque distribution of each wheel, especially with independent wheel drive electric vehicles. The intended vehicle path upon driver steering input is heavily depending on the instantaneous vehicle speed, body side slip and yaw rate of a vehicle, which can directly affect the steering effort of driver. In this paper, we propose a dynamic curvature controller (DCC) by applying a the dynamic curvature of the path, derived from vehicle dynamic state variables; yaw rate, side slip angle, and speed of a vehicle. The proposed controller, combined with DYC and wheel longitudinal slip control, is to utilize the dynamic curvature as a target control parameter for a feedback, avoiding estimating the vehicle side-slip angle. The effectiveness of the proposed controller, in view of stability and improved handling, has been validated with numerical simulations and a series of experiments during cornering engaging a disturbance torque driven by two rear independent in-wheel motors of a 4WD micro electric vehicle.

KEY WORDS : Direct yaw-moment control, Dynamic curvature, Stability, Handling

1. INTRODUCTION

Vehicle lateral dynamic control techniques such as direct yaw-moment control (DYC) and active front- and rear-wheel steering can improve the lateral dynamic performances by directly regulating yaw rate and tire slip angles and thus lateral tire forces, and/or by generating speed differentials or torque distributions, which are important in vehicle stability and maneuverability control under critical driving circumstances, such as aggressive cornering or near-limit driving performance conditions (Li *et al.*, 2008; Emirler *et al.*, 2015; Kim *et al.*, 2015a, 2015b; Jeong *et al.*, 2015). The fundamental DYC adopts the yaw moment observer by estimating the yaw rate, which is difficult to be measured. Using the yaw moment observer, the controller compensates the disturbance applied to the EV to keep the vehicle follow the reference trajectory. When the yaw rate is not the same as the desired yaw rate for cornering, the yaw moment observer finds the differences between actual and desired value of yaw rate. The perspective of DYC control is to provide a feedback of the difference of yaw rate for desired cornering regardless of disturbances.

Numerous control methods applying DYC have been proposed and verified in vehicle lateral dynamic performance improvement to assist drivers in enhancing cornering and straight-line stability on slippery roads and in unfavorable road conditions (Raksincharoensak *et al.*, 2008). For micro electric vehicles (MEVs) with in-wheel motor application, an electric differential system is widely used (Okajima *et al.*, 2010). Combined with independently controlled four in-wheel motored vehicles, the stability of electric vehicles (EVs) especially can be improved by controlling the driving/braking forces from generated speed differential between left and right wheels, thus the yaw moment is controlled to minimize the side slip angle at a vehicle center of gravity (c.g.) (Okajima *et al.*, 2010). Recently numerous studies are reported to improve the vehicle stability and maneuverability by applying body slip angle fuzzy observer, parameter uncertainties for robust yaw moment control (Du *et al.*, 2010), sliding mode control (Zhou and Liu, 2010), and comprehensive unified approach or vehicle full-state estimation (Cho *et al.*, 2012; Yim, 2015; Van Ende *et al.*, 2015).

However, due to the difficulties on estimating the side slip angle or lateral velocity of the vehicle, current production vehicles are not equipped to measure the side slip angle directly. Thus, the side slip angles are estimated

*Corresponding author. e-mail: insoo.suh@kaist.ac.kr

for vehicle control purposes for lateral dynamic stability and steer-by-wire or brake-by-wire system development, which require full vehicle dynamic state feedback (Mokhiamar and Abe, 2002). Common techniques for estimating side slip angle are integrating on-board inertial sensors or using a physical model as an observer. While these approach have applied to actual vehicle dynamics control, both has some fundamental errors, such as accumulated sensor errors and unrealistic measurements from road grade or bank angle, etc., while estimating with a physical vehicle model can be sensitive to changes in the vehicle parameters and inaccuracy on slippery road surfaces, etc.

We propose to apply, called as a dynamic curvature, to be applied as a main control target parameter (Jang *et al.*, 2015). By introducing the dynamic curvature as a main control parameter in the proposed dynamic curvature control (DCC) system, it will eliminate the necessity of measuring the vehicle side slip angle, which can be a unique approach from conventional DYC systems. In this case, the measured dynamic curvature can be obtained from an on-board IMU (inertial motion unit), while the reference dynamic curvature is set as the curvature of the vehicle path of the neutral steering case. An IMU is the basic on-board equipment for proposed DCC system. The dynamic curvature can be measured relatively easily, compared with estimating the vehicle sideslip angle, which will be described in this paper.

2. VEHICLE LATERAL DYNAMICS FOR DCC DURING CORNERING

2.1. Lateral Dynamics during Cornering

As shown in Figure 1, the lateral motion dynamics of a vehicle can be simplified as a bicycle model with two degrees of freedom by neglecting the force differences between left and right wheels (Rajamani, 2005). From the model, the equations of lateral motion can be derived as:

$$mv \left(\frac{d\beta}{dt} + \gamma \right) = 2(f_f + f_r) \quad (1)$$

$$I \frac{d\gamma}{dt} = M_z + M_t + M_d \quad (2)$$

where f_r and f_f are the lateral forces of front and rear tires, respectively, β is the vehicle side slip angle at the vehicle

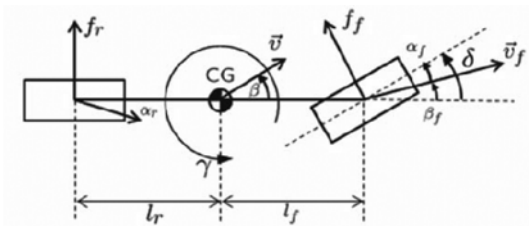


Figure 1. Bicycle model of the vehicle.

center of gravity (c.g. or CG), γ is the yaw rate, M_z is the motor torque moment from differential force, M_t is the torque moment from the lateral force of tire, M_d is a disturbance torque moment, and I is the yaw moment of inertia of the vehicle. For simplicity of analysis and verification, the longitudinal slip of tires or roll-over motions are not included in this paper. It is also assumed that the lateral force on the tire is generally proportional to tire slip angle for small slip angles. Side slip angles of each tire are approximated with the side slip angle of vehicle body. Using the above equations, the lateral dynamics of side slip angle and yaw rate can be derived as follows (Rajamani, 2005):

$$\dot{x} = A(v_x)x + B(v_x)u, \quad (3)$$

$$x = \begin{bmatrix} \beta \\ \gamma \end{bmatrix}, u = \begin{bmatrix} \delta \\ M_z \end{bmatrix},$$

$$A(v_x) = \begin{bmatrix} -\frac{2(C_f + C_r)}{mv_x} & -1 - \frac{2(l_f C_f - l_r C_r)}{mv_x^2} \\ -\frac{2(l_f C_f - l_r C_r)}{I} & -\frac{2(l_f^2 C_f + l_r^2 C_r)}{Iv_x} \end{bmatrix},$$

$$B(v_x) = \begin{bmatrix} \frac{2C_f}{mv_x} & 0 \\ \frac{2l_f C_f}{I} & \frac{1}{I} \end{bmatrix}$$

It follows from Equation (3) that the transfer functions of steering angle and state variables are obtained such that

$$\frac{\beta(s)}{\delta(s)} = \frac{g_{b1}s + g_{b0}}{s^2 + a_1s + a_2}, \quad (4)$$

$$\frac{\gamma(s)}{\delta(s)} = \frac{g_{f1}s + g_{f0}}{s^2 + a_1s + a_2}, \quad (5)$$

$$\frac{\gamma(s)}{M_z(s)} = \frac{g_{m1}s + g_{m0}}{s^2 + a_1s + a_2}, \quad (6)$$

where $g_{b1} = \frac{2C_f}{mv_x}$, $g_{b0}(v_x) = -\frac{2l_f C_f}{I} + \frac{4l_f LC_f C_r}{mIv_x^2}$,

$$g_{f1} = \frac{2l_f C_f}{I}, \quad g_{f0}(v_x) = \frac{4LC_f C_r}{mIv_x}, \quad g_{m1} = \frac{1}{I},$$

$$g_{f0}(v_x) = \frac{4LC_f C_r}{mIv_x}, \quad g_{m0}(v_x) = \frac{2(C_f + C_r)}{mIv_x},$$

$$a_1 = \frac{2(C_f + C_r)}{mv_x} + \frac{2C_f}{Iv_x}, \text{ and}$$

$$a_2 = \frac{4L^2 C_f C_r}{mIv_x^2} - \frac{2(l_f C_f - l_r C_r)}{I}.$$

α_f, α_r : tire slip angle at front and rear

β : body side slip angle at vehicle c.g.

- β_f, β_r : tire side slip angle at front and rear
 δ : steering angle input by driver
 \vec{v} : velocity vector at vehicle c.g.
 v_x : longitudinal velocity
 m : mass of the vehicle
 l_f, l_r : distances between the vehicle c.g. and front or rear wheel axle
 L : wheelbase of the vehicle ($= l_f + l_r$)
 C_f, C_r : stiffness at rear and front tire

With the simplified 2-d.o.f. model, the lateral dynamic equations can be described with two state variables and two inputs. Specifically, the yaw rate, γ and side slip angle, β can be controlled by steering angle, δ and motor torque moment M_z . The objective of a DYC in general is to maintain vehicle stability via regulating the vehicle yaw rate. It is emphasized here that the differential torque of two rear motors is utilized for DYC aside from steering angle change. It is believed that the differential torque makes the vehicle's cornering effort more less than relying just on side slip angle of the front wheel. Sub-headings are numbered as above. Subsections are numbered sequentially.

2.2. Dynamic Control for Neutral Steering

Vehicle handling conditions during cornering will be different depending on vehicle speeds and difference in tire stiffness, etc. They are classified as under-steering, neutral steering, and over-steering, as shown in Figure 2. A normal vehicle tends to be under-steering making the radius of curvature larger, if it is accelerated with a constant steering angle. The side slip angle in case of under-steering is illustrated in Figure 2.

The vehicle dynamic motions during a neutral steering can be described from Equation (3) by letting v_x a constant, v_c .

$$\dot{\bar{x}} = A(v_c)\bar{x} + B(v_c)u \quad (7)$$

$$\bar{x} = \begin{bmatrix} \beta \\ \gamma \end{bmatrix}, u = \begin{bmatrix} \delta \\ M_z \end{bmatrix},$$

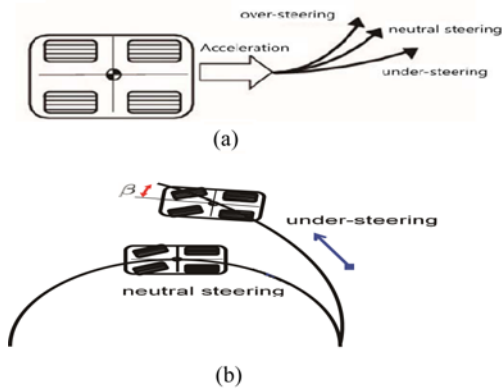


Figure 2. Vehicle dynamic motions during cornering: (a) Vehicle handling conditions; (b) Side slip angle during under-steering.

where v_c is a constant longitudinal velocity, δ is a steering angle for neutral steering, and the variables with ‘-’ indicate the variables while the vehicle is under neutral steering for a constant radius.

3. CURVATURE DETERMINATION AND DYNAMIC CURVATURE FOR CONTROL

3.1. Curvature of Vehicle Driving Path

There are many ways to measure the curvature during vehicle motion. Firstly, the curvature can be derived from the dynamic steady state model with the following assumptions, that the sum of the lateral forces at front and rear tires is the same as the centrifugal force, and that the torque moment by the lateral force is zero. When the vehicle drives following a curve with a constant radius, the curvature should be equal to (Rajamani, 2005);

$$\frac{1}{R} = \frac{\delta}{L + mv_x^2 \left(\frac{l_f C_r - l_r C_f}{2C_f C_r L} \right)} \quad (8)$$

where the steering angle and longitudinal speed can be measured by on-board sensors in a vehicle. However, a drawback of this approach is that the tire stiffness, C_r and C_f are not readily available, so they need to be estimated by other methods. Also, there can be possible errors because this curvature formula is derived from the steady state model.

3.2. Dynamic Curvature

In this work, we introduce a dynamic curvature variable as a main control parameter within a DYC system. When the radius of vehicle cornering path is R , the instantaneous curvature of the vehicle driving path, k can be expressed, as introduced (Okajima *et al.*, 2010);

$$k = \frac{\dot{\beta} + \gamma}{v_x} \quad (9)$$

The variable k can be considered as a measure of the instantaneous dynamic curvature of vehicle path, so we name it here as a ‘dynamic curvature’. Note that k is conveniently measured in practice since yaw rate, γ is directly available from a yaw rate sensor and time-derivative of the side slip angle, $\dot{\beta}$ can be calculated from an on-board IMU sensor. The dynamic curvature is a characteristic variable of vehicle dynamics during cornering. Let a total lateral vehicle movement angle defined by

$$\varphi = \beta + \int_0^t \gamma d\tau.$$

4. PROPOSED DYNAMIC CURVATURE CONTROL (DCC) SYSTEM

4.1. Proposed DCC Control with Reference Neutral Steering Subheading

The control algorithm and resultant performances of the direct yaw moment control method based on the yaw

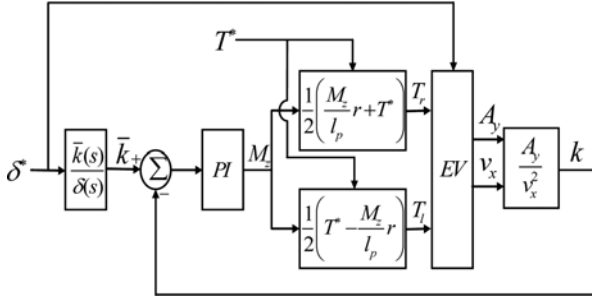


Figure 3. Block diagram of the proposed DCC control algorithm.

moment observer have been presented in Li *et al.* (2008), Kim *et al.* (2015a, 2015b) and Jeong *et al.* (2015). The typical DYC algorithm utilizes the yaw rate as a feedback variable, to stabilize the vehicle lateral dynamic motion. Note that the typical DYC's focus on regulating the yaw rate so that they may fail to obtain neutral steering trajectory when the lateral tire slip conditions are not even or changing. More specifically, DYC controls the yaw rate only, the vehicle maneuverability or the dynamic curvature control is not directly reflected during steering motion.

In this work, the dynamic curvature is a target variable to be controlled instead of yaw rate. It should be emphasized that the side slip angle change, being a major influential element to determine a circular motion, is included in the dynamic curvature. Therefore, the DCC enables the vehicle to track a neutral trajectory better than DYC. Note that the lateral acceleration which is equal to $(\gamma + \dot{\beta})v_x$ directly obtainable from an IMU sensor. Therefore, the dynamics curvature is measured as

$$k = \frac{\gamma + \dot{\beta}}{v_x} = \frac{A_y}{v_x^2}. \quad (10)$$

Note that the DCC is advantageous in implementation since the dynamic curvature, k is relatively easily measured for feedback control without monitoring or estimating the side slip angle, β separately.

Figure 3 shows the proposed DCC block diagram based on measured dynamics curvature, which will be described in below. A steering reference value, δ^* is applied as a command value.

5. SIMULATION AND TEST RESULTS

5.1. Simulation Results

An EV with two sets of independent motors at rear wheels (Suh *et al.*, 2013, 2015; Lee *et al.*, 2014) is accelerated from 18 km/h to 30 km/h for 20 seconds for a simulation purpose. The velocity of the reference model is chosen as $v_r = 10$ km/h. Initial position of the vehicle is set as the coordinate of (0, 0) for plotting purpose. For the simulation and experimental purpose, the disturbance torque is applied at the front left tire. The disturbance torque moment

Table 1. Vehicle parameters for simulation.

Parameter	Description	Value
C_f	Front tire stiffness	22,000 N/rad
C_r	Rear tire stiffness	26,000 N/rad
m	Vehicle mass	650 kg
l_f	Disyance bet. CG and front tire	0.68 m
l_r	Distance bet. CG and rear tire	0.59 m

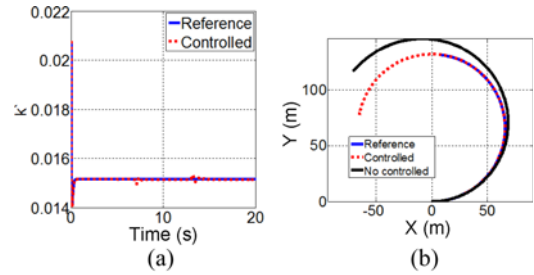


Figure 4. Simulation results: (a) Dynamic curvature k ; (b) Vehicle trajectory.

applied from 7.5 second to 12.5 second with a value of 50 Nm at the front left tire, which simulates the vehicle velocity is abruptly changing during the cornering, possibly caused by strong wind and road friction difference between left and right, etc. By using the reference law, the reference dynamic curvature, k is determined to keep the vehicle's desired trajectory with a constant speed, as shown in Figure 4 (a). We can see that the vehicle's radius of curvature with the proposed control follows the reference trajectory, i.e. the neutral steering case, while the radius of the vehicle path without the control becomes larger as the vehicle velocity is increased, as shown in Figure 4 (b).

5.2. Test Results

Figure 5 shows the experimental environment, such as the test track, the micro electric vehicle with two rear wheel independent control, driving test scene, and the on-board GPS receiver. The specification of the test track can be explained with the vehicle trajectory as shown in Figure 5.



Figure 5. Experimental environment: (a) Test track for driving test; (b) Subject vehicle for testing with two independent motor control at rear wheels.

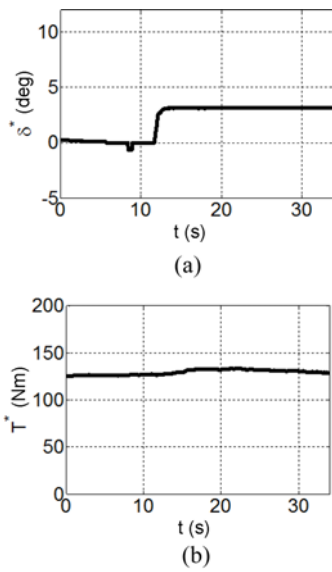


Figure 6. Vehicle control input during the experiment when the controller is turned on: (a) Steering angle; (b) Torque at rear wheels.

The vehicle, as described (Suh *et al.*, 2013; Lee *et al.*, 2014), of which specifications are shown in Table 1, is driven along the line in Figure 5 (a).

The actually engaged steering angle input and torque input during this experiment are shown in Figure 6. Figure 7 shows the measured vehicle trajectory with the dynamic curvature controller turned on. Differently from no curvature control case, the trajectory keeps the constant curvature, as if the vehicle maneuvers under neutral steering. The measured instantaneous lateral acceleration of the subject vehicle during cornering is shown in Figure 8 (a) and the corresponding measured side slip angle is shown in Figure

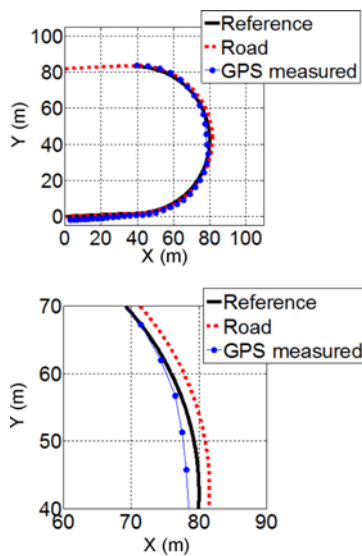


Figure 7. Experimental results when the controller is turned on: Measured vehicle trajectory.

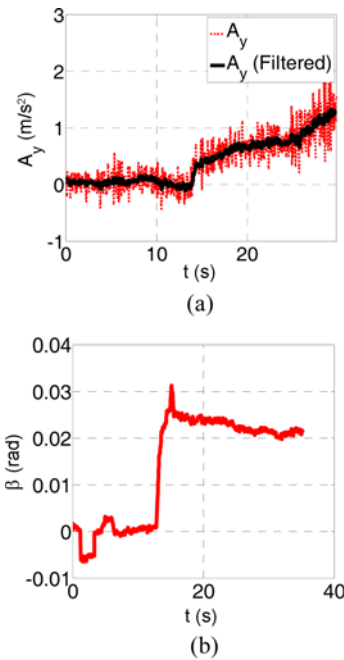


Figure 8. Experimental results when the controller is turned on: (a) Vehicle lateral acceleration; (b) Vehicle side slip angle.

8 (b), respectively. In addition, the measured instantaneous torque output from the left and right motor are shown in Figure 9 (a) and the corresponding dynamic curvature in Figure 9 (b). As the longitudinal speed increases, the lateral acceleration increases also due to the centrifugal forces

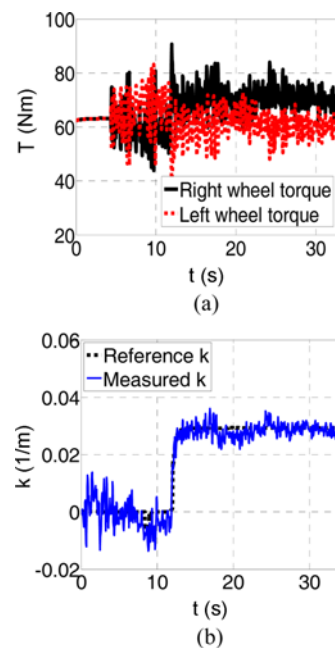


Figure 9. Experimental results when the controller is turned on: (a) Measured torque of each motor; (b) Measured and reference dynamic curvature k .

during cornering. But the dynamic curvature controller provides a feedback signal of the lateral acceleration to stay at the constant curvature radius.

6. CONCLUSION

The direct yaw rate control (DYC) system introducing the defined parameter of the dynamic curvature, k , which is called in dynamic curvature control (DCC) system, is proposed and verified the effectiveness with the simulation and a series of experiment in this paper. The instantaneous dynamic curvature can be obtained from the measured lateral acceleration and longitudinal speed by an on-board IMU easily.

The measurable dynamic curvature, k , is utilized as a feedback parameter during vehicle cornering motion especially when the speed of the vehicle is varied, emphasizing the dynamic handling as well as the vehicle dynamic stability.

The dynamic curvature of the vehicle path with the control system maintained the constant radius of curvature, as the reference model of neutral steering during the cornering, even with the disturbance engaged, which proved the effectiveness of vehicle handling as well as the dynamic stability.

ACKNOWLEDGEMENT—The authors would like to thank you for the support from the Korean Ministry of Science, ICT and Future Planning and the Korean Ministry of Land, Infrastructure and Transport.

REFERENCES

- Cho, W., Choi, J., Kim, C., Choi, S. and Yi, K. (2012). Unified chassis control for the improvement of agility, maneuverability, and lateral stability. *IEEE Trans. Vehicular Technology* **61**, **3**, 1008–1020.
- Du, H., Zhang, N. and Dong, G. (2010). Stabilizing vehicle lateral dynamics with considerations of parameter uncertainties and control saturation through robust yaw control. *IEEE Trans. Vehicular Technology* **59**, **5**, 2593–2597.
- Emirler, M. T., Kahraman, K., Senturk, M., Acar, O. U., Aksun Guvenc, B., Guven, L. and Efendioglu, B. (2015). Lateral stability control of fully electric vehicles. *Int. J. Automotive Technology* **16**, **2**, 317–328.
- Jang, Y., Lee, M., Suh, I. and Nam, K. (2015). Lateral handling improvement with dynamic curvature control for an independent rear wheel drive EV. *Proc. EVS28, KINTEX, Korea*.
- Jeong, C. H., Kim, J. Y. and Jung, D. H. (2015). Research on vehicle stability technology based on wheel force. *Int. J. Automotive Technology* **16**, **3**, 435–445.
- Kim, H., Lee, S. and Hedrick, J. K. (2015a). Active control for handling performance improvement by using traction force. *Int. J. Automotive Technology* **16**, **3**, 457–464.
- Kim, K. W., Lee, S. B., Park, C. S. and Yi, K. (2015b). Estimation of lateral distribution under parameter uncertainties. *Int. J. Automotive Technology* **16**, **3**, 427–433.
- Lee, M., Lee, K., Hwang, K. and Suh, I. (2014). Development of a foldable micro electric vehicle for future urban driving with intelligent control. *IEEE 17th Int. Conf. Intelligent Transportation Systems*, 2486–2491.
- Li, D., Du, S. and Yu, F. (2008). Integrated vehicle chassis control based on direct yaw moment, active steering and active stabiliser. *Vehicle System Dynamics* **46**, **Supplement 1**, 341–351.
- Mokhiamar, O. and Abe, M. (2002). Active wheel steering and yaw moment control combination to maximize stability as well as vehicle responsiveness during quick lane change for active vehicle handling safety. *Proc. Institution of Mechanical Engineers, Part D: J. Automobile Engineering* **216**, **2**, 115–124.
- Okajima, H., Yonaha, S., Matunaga, N. and Kawaji, S. (2010). Direct yaw-moment control method for electric vehicles to follow the desired path by driver. *Proc. SICE Annual Conf.*, 642–647.
- Rajamani, R. (2012). *Vehicle Dynamics and Control*. 2nd edn. Springer. New York, USA.
- Raksincharoensak, P., Mizushima, T. and Nagai, M. (2008). Direct yaw moment control system based on driver behavior recognition. *Vehicle System Dynamics* **46**, **Supplement 1**, 911–921.
- Suh, I., Cho, D., Hong, S., Jung, S., Lee, B., Miller, J., Risch, F., Shinohara, N. and Turki, F. (2015). *Wireless Charging Technology and the Future of Electric Transportation*. SAE International. Warrendale, Pennsylvania, USA.
- Suh, I., Hwang, K., Lee, M. and Kim, J. (2013). In-wheel motor application in a 4WD electric vehicle with foldable body concept. *IEEE Int. Electric Machines & Drives Conf.*, 1307–1312.
- Van Ende, K., Kucukay, F., Henze, R., Kallmeyer, F. and Hoffman, J. (2015). Vehicle and steering dynamics in the context of on-centre handling. *Int. J. Automotive Technology* **16**, **5**, 751–763.
- Yim, S. J. (2015). Unified chassis control with electronic stability control and active front steering for understeering prevention. *Int. J. Automotive Technology* **16**, **5**, 775–782.
- Zhou, H. and Liu, Z. (2010). Vehicle yaw stability-control system design based on sliding mode and backstepping control approach. *IEEE Trans. Vehicular Technology* **59**, **7**, 3674–3678.